

Quantitative Flow Imaging in Human Umbilical Vessels In Utero Using Nongated 2D Phase Contrast MRI

Uday Krishnamurthy, PhD,^{1,2} Brijesh K. Yadav, MS,^{1,2} Pavan K. Jella, MS,¹
Ewart Mark Haacke, PhD,^{1,2} Edgar Hernandez-Andrade, MD, PhD,^{3,4}
Swati Mody, MD,¹ Lami Yeo, MD,^{3,4} Sonia S. Hassan, MD,^{3,4}
Roberto Romero, MD, DMedSci,^{3,5,6,7} and Jaladhar Neelavalli, PhD^{1,2*}

Background: Volumetric assessment of afferent blood flow rate provides a measure of global organ perfusion. Phase-contrast magnetic resonance imaging (PCMRI) is a reliable tool for volumetric flow quantification, but given the challenges with motion and lack of physiologic gating signal, such studies, in vivo on the human placenta, are scant.

Purpose: To evaluate and apply a nongated (ng) PCMRI technique for quantifying blood flow rates in utero in umbilical vessels.

Study Type: Prospective study design.

Study Population: Twenty-four pregnant women with median gestational age (GA) 30 4/7 weeks and interquartile range (IQR) 8 1/7 weeks.

Field Strength/Sequence: All scans were performed on a 3.0T Siemens Verio system using the ng-PCMRI technique.

Assessment: The GA-dependent increase in umbilical vein (UV) and arterial (UA) flow was compared to previously published values. Systematic error to be expected from ng-PCMRI, in the context of pulsatile UA flow and partial voluming, was studied through Monte-Carlo simulations, as a function of resolution and number of averages.

Statistical Tests: Correlation between the UA and UV was evaluated using a generalized linear model.

Results: Simulations showed that ng-PCMRI measurement variance reduced by increasing the number of averages. For vessels on the order of 2 voxels in radius, partial voluming led to 10% underestimation in the flow. In fetuses, the average flow rates in UAs and UV were measured to be 203 ± 80 ml/min and 232 ± 92 ml/min and the normalized average flow rates were 140 ± 59 ml/min/kg and 155 ± 57 ml/min/kg, respectively. Excellent correlation was found between the total arterial flow vs. corresponding venous flow, with a slope of 1.08 ($P = 0.036$).

Data Conclusion: Ng-PCMRI can provide accurate volumetric flow measurements in utero in the human umbilical vessels. Care needs to be taken to ensure sufficiently high-resolution data are acquired to minimize partial voluming-related errors.

Level of Evidence: 2

Technical Efficacy: Stage 1

J. MAGN. RESON. IMAGING 2018;48:283–289.

The growth and development of the human fetus is supported through an effective maternofetal circulation and nutrient exchange. Assessment of fetoplacental hemodynamics using ultrasound Doppler velocimetry parameters such as pulsatility index (PI), resistance index (RI), peak velocities during

diastole and systole (S/D ratio), or the presence/absence of notch in the uterine artery blood flow waveform is performed routinely during pregnancy.^{1,2} Indeed, in cases of severe fetal growth restriction (FGR), increased umbilical artery PI is found to be a useful indicator of fetal distress and a good

View this article online at wileyonlinelibrary.com. DOI: 10.1002/jmri.25917

Received Jul 26, 2017, Accepted for publication Nov 14, 2017.

*Address reprint requests to: J.N., Department of Radiology, Wayne State University School of Medicine, 4201 St. Antoine, Detroit, MI 48201.

E-mail: jneelava@med.wayne.edu

From the ¹Department of Radiology, Wayne State University School of Medicine, Detroit, Michigan, USA; ²Department of Biomedical Engineering, Wayne State University College of Engineering, Detroit, Michigan, USA; ³Perinatology Research Branch, NICHD/NIH/DHHS, Bethesda, Maryland, and Detroit, Michigan, USA; ⁴Department of Obstetrics and Gynecology, Wayne State University School of Medicine, Detroit, Michigan, USA; ⁵Department of Obstetrics and Gynecology, University of Michigan, Ann Arbor, Michigan, USA; ⁶Department of Epidemiology and Biostatistics, Michigan State University, East Lansing, Michigan, USA; and ⁷Center for Molecular Medicine and Genetics, Wayne State University, Detroit, Michigan, USA

predictor of adverse perinatal outcome.^{3,4} While these indices characterize blood flow dynamics, they do not provide estimates of volumetric blood flow rates in the umbilical vessels. Quantifying volumetric blood flow rates in major fetoplacental vessels could help in evaluating bulk organ perfusion, which is an important physiologic parameter.

Doppler ultrasound (US) may be used for such assessment. However, the accuracy and repeatability of Doppler-based volumetric flow measurements in fetal vessels is affected by factors like insonation angle, the variability in the estimation of the vessel area, and the absence of accounting for the spatial velocity profile.⁵⁻⁷ Furthermore, flow measurements based on Doppler estimations may not be possible to obtain when vessels are located in close proximity to a highly echogenic tissue such as bone, or in cases of reduced amniotic fluid (oligohydramnios). Magnetic resonance imaging (MRI) provides a strong adjunct to US in fetal diagnostic imaging^{8,9} and offers quantitative imaging capability with large fields-of-view, at high resolutions that is relatively operator-independent. Furthermore, phase contrast MRI (PCMRI) is one of the most accurate methods for measuring *in vivo* blood flow rates and is routinely used clinically in neonates, children, and in adult subjects for blood or cerebrospinal fluid flow quantification.¹⁰⁻¹² In addition, evaluation of bulk organ perfusion or oxygen delivery and/or consumption rates *in utero* would also require the information about the blood flow rates in fetoplacental vessels using MRI. Such approaches are increasingly becoming important in the study of the most frequent obstetric complications.¹³

Studies applying PCMRI for evaluating fetal and/or placental blood flow, however, are scant, perhaps due to 1) the lack of physiologic gating signal (fetal echocardiography or fetal pulse monitor) within the MRI system that facilitates synchronization of data acquisition for time-resolved flow quantification; and 2) fetal motion. Specifically, the latter aspect necessitates fast imaging methods that minimize chances of data corruption from fetal movements. To address the former aspect, approaches like data-driven self-gating,¹⁴ and the use of MR-safe fetal cardiocography equipment, are active areas of research.^{15,16} However, application of these methods requires either complex reconstruction algorithms or custom hardware. Furthermore, due to their long acquisition times, these techniques are prone to fetal motion, which precludes useful measurement. Alternatively, nongated PCMRI (ng-PCMRI) is a fast method that can map time-averaged velocity in a spatially resolved manner, without the necessity of any gating signal. It thus enables measurement of average blood flow rates for conditions found *in vivo*.¹⁷ Given the above-mentioned advantages of ng-PCMRI, in this work we aimed to evaluate its applicability towards quantifying blood flow rates *in utero* in human umbilical vessels.

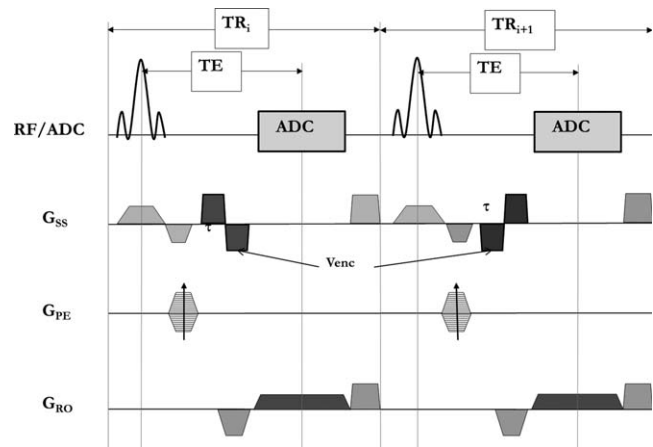


FIGURE 1: Sequence diagram of the nongated phase contrast MRI (ng-PCMRI) showing the continuous acquisition without the need for any trigger signal. RF, radio frequency excitation pulse; ADC, analog to digital converter; G_{ss} , slice select gradient; G_{PE} , phase encoding gradient; G_{RO} , readout gradient.

Materials and Methods

Nongated PC-MRI Sequence

The conventional 2D time-resolved PC imaging sequence with Cartesian data sampling was modified to phase encode without the gating signal. The bipolar velocity encoding was implemented with the positive and negative polarity occurring in consecutive repeat-times (TR_i and TR_{i+1}), as shown in Fig. 1. Flow encoding is applied along the slice direction and two images are obtained as the output of the sequence: one with positive and the other with negative bipolar velocity encoding. The final ng-PCMRI image is obtained by complex dividing the positive and negative velocity encoding data and taking the resultant phase image.

Numerical Simulations for Umbilical Flow Measurement

In ng-PCMRI, phase-encoding occurs over different cardiac phases, providing an average velocity measure in the final image. In the case of pulsatile flow, the vessel phase varies from view-to-view (ie, phase encode to phase encode). This could introduce a bias in the average velocity measured, depending on the relative position of the phase-encode order and the pulsatile velocity-time curve. Averaging over multiple measurements can reduce such variability.¹⁸

To understand the nature of such errors for a typical velocity-time profile of flow in the umbilical vessels, we performed numerical simulations using a 2D digital flow phantom. For steady flow conditions without any pulsatility, as in the umbilical vein, ng-PCMRI does not lead to any systematic quantification error.¹⁸ Hence, the velocity-time profile of umbilical arteries, which have pulsatile flow, was considered in these simulations. Two sets of simulations were carried out to assess the degree of error in flow: 1) due to the typical variability in fetal heart rate during data acquisition¹⁹; and 2) due to partial volume effects. A laminar spatial flow profile was considered.²⁰ Anonymized umbilical artery blood flow velocity waveform from a normal fetus in third trimester was obtained from the local obstetrical care center. Using this waveform, a fetal blood flow velocity curve was generated for the entire duration of a simulated ng-PCMRI acquisition, with a velocity value available for each TR of the acquisition.

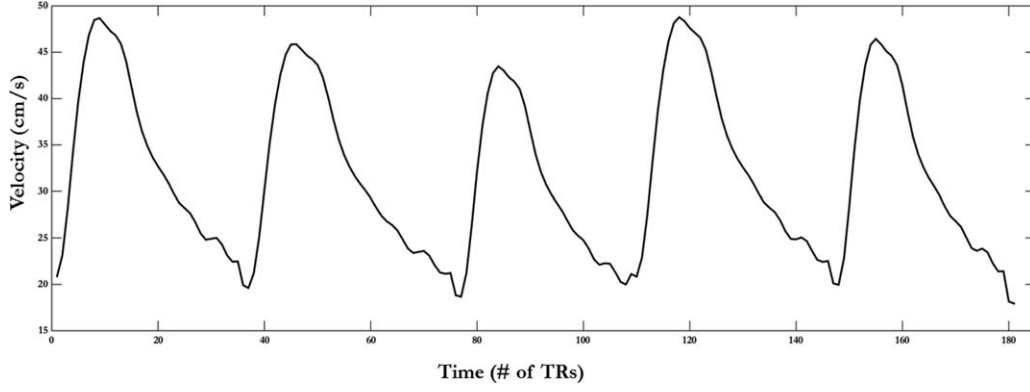


FIGURE 2: A section of the velocity–time curve generated after introduction of the beat-to-beat random variation in amplitude ($\pm 10\%$) and period (± 50 msec) of the fetal cardiac cycle.

In generating this waveform, for multiple repeated simulations (see N_{sim} parameter, below), typical fetal heart rate variability and amplitude variation in the flow were considered. Gaussian variability in the fetal ECG period was introduced with a mean R-to-R interval value of 445 msec and a standard deviation of 50 msec. Similarly, the peak amplitude of the velocity–time curve was also varied with a mean peak value of 45 cms/sec and standard deviation of 4.5 cms/sec (10%). Figure 2 illustrates a section of the velocity–time curve generated for digital simulation of ng-PCMRI.

The digital flow phantom consisted of two concentric cylinders, set up within a 256×256 matrix. The inner cylinder, which represented the vessel (radius 16 pixels), was embedded in a larger outer cylinder (radius 103 pixels) simulating the background tissue. Arbitrary amplitudes of 100 and 25 units were assigned to the vessel and background, respectively, which defined the magnitude $M(x,y)$. A laminar flow profile within the vessel lumen was simulated using Eq. (1):

$$v(x) = V_{\text{max}} \left(1 - \frac{r}{R}\right)^2 \quad (1)$$

where r is the radial distance of a point in the vessel from its center and R is the radius of the vessel.

Similar to the actual data acquisition procedure in MR, velocities corresponding to each pair of consecutive TRs were taken and assigned to the vessel to generate the positive and negative bipolar phase-encode lines. The following equations summarize this process.

$$p(k_{pe,j}) = FT[M(x,y) \cdot e^{i\varphi_{p,vessel}(r,t)}]_j \quad (2)$$

$$n(k_{pe,j}) = FT[M(x,y) \cdot e^{i\varphi_{n,vessel}(r,t)}]_j$$

$$\varphi_{p,vessel}(t) = \begin{cases} \left(\pi \cdot \frac{v(r,t)}{V_{enc}}\right) - \text{Inside the vessel} \\ 0 - \text{In the background tissue} \end{cases} \quad (3)$$

$$\varphi_{n,vessel}(t) = \begin{cases} -\left(\pi \cdot \frac{v(r,t)}{V_{enc}}\right) - \text{Inside the vessel} \\ 0 - \text{In the background tissue} \end{cases} \quad (4)$$

Here, $p(k_{pe,j})$ and $n(k_{pe,j})$ are the k -space lines corresponding to the positive and negative bipolar velocity encoding; j indicates the j^{th}

phase encode line; $\varphi_{p,vessel}(r,t)$ and $\varphi_{n,vessel}(r,t)$ are the vessel phase corresponding to the positive and negative bipolar lobe encoding, respectively. V_{enc} is the velocity that corresponds to a phase of π . Gaussian noise was added during the k -space generation such that the signal-to-noise ratio (SNR) in the background tissue was 5:1. A V_{enc} value of 50 cm/sec was used. Short-term averaging (N_{avg} = number of averages) was simulated similarly, but with consecutive pairs of TRs now corresponding to the same phase encode step, for a duration of $2 \cdot \text{TR} \cdot N_{\text{avg}}$. The generated N_{avg} phase-encode lines for a given phase encode step were averaged (positive and negative encoding lines separately). The final ng-PCMRI image was generated by complex dividing the images corresponding to positive and negative bipolar encodings according to:

$$I(x,y) = \frac{FT^{-1}[p(k)]}{FT^{-1}[n(k)]} \quad (5)$$

The simulation was carried out for averages, N_{avg} , ranging from 1 to 10 (step size = 1). Percent error in the velocity (or flow) from ng-PCMRI, relative to the corresponding theoretical average velocity, obtained from the input velocity–time curve, was then evaluated. The simulation was repeated, $N_{\text{sim}} = 300$ times, where in each instance a different heart rate variability and amplitude variation were introduced in the umbilical velocity–time curve. For a given N_{avg} , the standard deviation of the percent error, over the N_{sim} values, represented the systematic error expected from ng-PCMRI in the umbilical artery flow.

Large voxel sizes relative to the vessel size lead to partial volume effects and consequent errors in the measurement of velocity and vessel cross-sectional area (CSA). For assessing the influence of these factors in ng-PCMRI for pulsatile flow, a procedure similar to the one used by Jiang et al²⁰ was employed. Briefly, instead of starting with a matrix size of 256×256 , a larger matrix size is taken and condensed to the final matrix size of interest, by taking the central k -space region, to simulate partial voluming. Vessels of radii 2, 3, 4, 6, and 8 voxels in the final matrix size were simulated by starting with a vessel of size 32, 48, 64, 96, and 128, respectively, in a matrix size of 4096×4096 . Laminar flow profile as described earlier (Eq. (1)) was used and velocity and flow error in the final partial-volumed vessel was evaluated as a function of vessel diameter. Simulations were carried out for $N_{\text{avg}} = 6$ and $N_{\text{sim}} = 20$. In this assessment, the vessel CSA was measured

automatically using a simple intensity threshold corresponding to 85% of the peak signal within the lumen in the magnitude images.

Fetal Imaging

Pregnant women with singleton pregnancies, between the age of 18 to 38 years of age and who were between 19 and 40 weeks gestation, receiving care at Hutzel Women’s Hospital in Detroit, MI, were nonconsecutively recruited in this study. The imaging study was approved by the local Institutional Review Board (IRB) and was compliant with HIPAA regulations. All subjects imaged in this study were recruited in accordance with local IRB guidelines and written informed consent was obtained prior to the MRI scan. Subjects with uncomplicated pregnancy, assessed based on their routine US examination, were recruited. The criteria for uncomplicated pregnancy were: a normal anatomical evaluation of the fetus, umbilical artery pulsatility index <95th centile and estimated fetal weight before umbilical artery Doppler to be within the 10–90th centile for gestational age (GA). The fetal weight was estimated using the equation provided by Hadlock et al,²¹ which involved US-based evaluation of four fetal biometric parameters: biparietal diameter (BPD), head circumference (HC), abdominal circumference (AC), and femur length (FL).

Fetal MRI scans were performed with a 3.0T Siemens Verio scanner (Erlangen, Germany) with a 4-channel body flex array coil along with the spine coil. An additional 2-channel flex extremity receive coil was used in some patients with larger girth. As part of a larger study, ng-PCMRI data were acquired whenever possible. The umbilical vessels were first localized using a noncontrast, nonbreath-hold time-of-flight MRA sequence.²² Once the umbilical cord was localized, nontriggered phase contrast images using the modified sequence were acquired using the following parameters: repetition time (TR) of 14 msec, echo time (TE) of 7–9 msec, slice thickness of 3/4 mm, voxel size between (0.5–0.8) × (0.5–0.8) mm², and flip angle of 15°. The acquisition time for the sequence was 90 seconds for N_{avg} = 6. The energy deposited, measured as whole-body specific absorption rate (SAR), was consistently maintained below 0.5 W/kg. Whenever possible, within the limitations of time, acquisitions were repeated when fetal motion was encountered.

The ng-PCMRI data were first evaluated for data quality and those with significant motion artifacts, which precluded measurement, were excluded from analysis. Subsequent to this initial assessment, N = 24 cases were included for quantitative analysis in this study: median GA, 30 4/7 weeks and interquartile range (IQR), 8 1/7 weeks with a range of 24 weeks to 39 weeks and 5 days. Flow was quantified using an in-house software “flowQ” developed in MatLab (MathWorks, Natick, MA),²³ which allowed for drawing a manual region of interest (ROI). The analysis was carried out independently by two different observers (U.K. and B.K.Y.). The interrater agreement was statistically analyzed using the interclass correlation coefficient (ICC). The fetal weight assessment was performed within 1 week prior to the MRI scan. The blood flow rate per unit fetal weight was also calculated by normalizing the net umbilical flow measures (for arteries and vein) by the corresponding estimated fetal weight. Correlation between the total umbilical arterial flow (both arteries combined) vs. the flow in umbilical vein, across the 24 fetuses, was also statistically evaluated

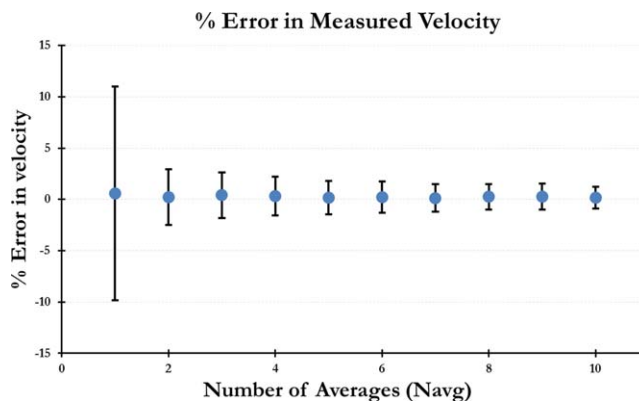


FIGURE 3: Error in the measured velocity as a function of number of averages (N_{avg}). Data were simulated using a representative umbilical artery waveform incorporating the beat-to-beat variations in amplitude and duration of the cardiac cycle.

using a generalized linear model. For all statistical tests, significance was defined by p < 0.05.

Results

Numerical Simulations

Figure 3 shows the mean percent error in the measured velocity and the corresponding standard deviation over N_{sim} = 300, as a function of N_{avg}. While the error itself is small, the variance in this error decreased with increasing N_{avg}. Given the mean error of 0.22% ± 1.5% for N_{avg} = 6, we chose this number for in vivo imaging as a reasonable trade-off between total imaging time and variance in the measurement.

Figure 4 plots the percent error in the measured velocity and flow for vessels ranging from radius 2 to radius 8 voxels for N_{avg} = 6 and N_{sim} = 20. Measurement error in velocity and flow decreased as the vessel size (in voxels) increased and percent error in flow was smaller than that in velocity. For a vessel radius of 2 voxels, the error in flow was measured to be 10% ± 0.4% and at radius 3 voxels, 7.2% ± 0.5%.

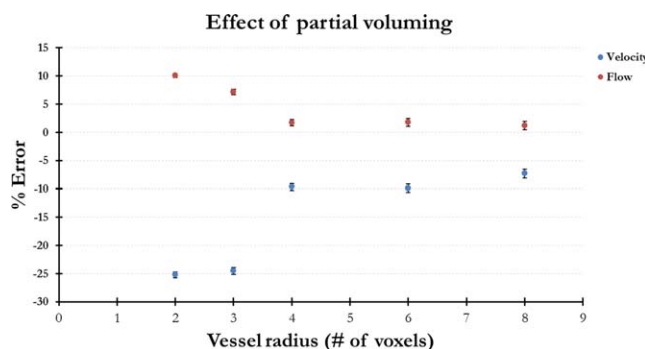


FIGURE 4: Error in the measured velocity and flow as a function of vessel diameter. While velocity error is larger than flow error, both errors decrease as vessel size increases. N_{sim} = 20, N_{avg} = 6.

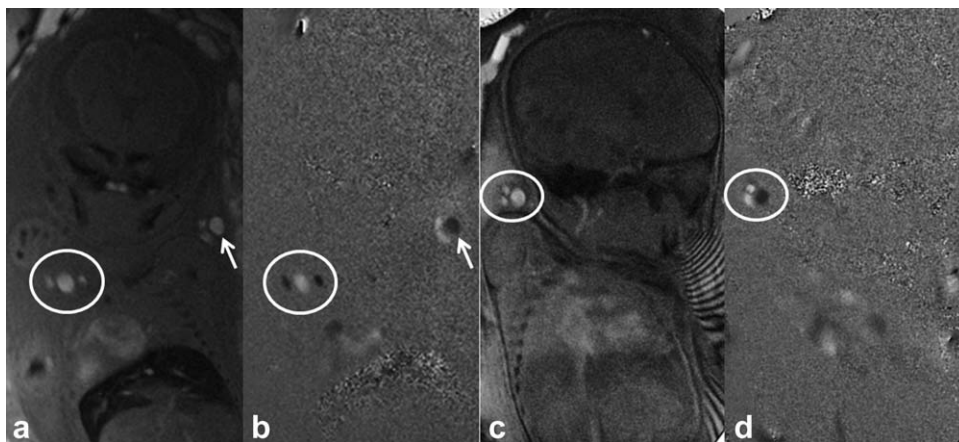


FIGURE 5: Magnitude (a,c) and the phase image (b,d) obtained from the ng-PCMRI. Representative images are shown from a second trimester fetus (left pair (a,b); GA, 25 4/7 weeks) and a third trimester (right pair (c,d); GA, 35 1/7 weeks). Note the hyper-intense phase in the two umbilical arteries vs. the hypo-intense phase in the umbilical vein.

Fetal Umbilical Imaging

Figure 5 shows the representative magnitude and phase images from ng-PCMRI that show the umbilical vessels where the opposite flow in the arteries and veins is indicated by the opposite phase signature in the phase images. The average flow across the 24 fetuses, in the two umbilical arteries combined, was 203 ± 80 ml/min and the corresponding flow in the umbilical vein was 232 ± 92 ml/min with a range of 68–378 ml/min and 62–420 ml/min, respectively. Excellent interobserver agreement was found in umbilicus flow and velocity measurements: ICC-flow: 1) umbilical arteries $r: 0.86$ ($P < 10^{-6}$) and 2) umbilical vein $r: 0.96$ ($P < 10^{-10}$); ICC-velocity: 3) umbilical artery 1 $r: 0.93$ ($P < 10^{-10}$); umbilical artery 2 $r: 0.79$ ($P < 10^{-06}$); and 4) umbilical vein $r: 0.97$ ($P < 10^{-10}$). The flow in both the artery and the vein increased with increasing GA (Fig. 6). Total arterial flow (artery1 + artery2) vs. corresponding total venous flow correlated well with each other with a slope of 1.08 ($P = 0.036$) (Fig. 7). The average blood flow per unit weight of the fetus, across all the fetuses, was 140 ± 59 ml/kg per min and 155 ± 57 ml/kg per min in the umbilical artery and vein, respectively.

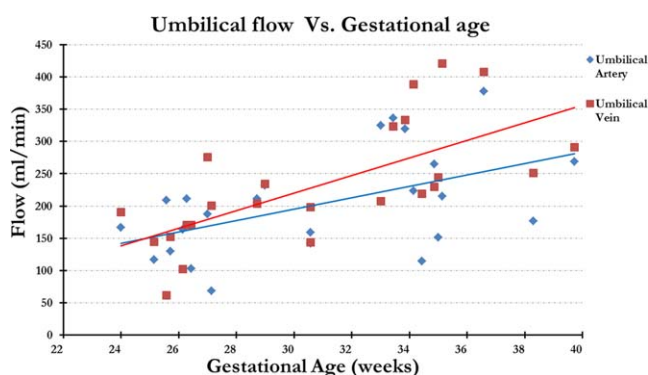


FIGURE 6: Arterial and venous flow plotted across gestational age. Both show an expected increasing trend with respect to gestational age; however, the arterial flow appears slightly underestimated.

Discussion

We have shown that measuring the average umbilical blood flow rate in vivo using nongated PCMRI is possible. Using Monte-Carlo simulations, we assessed the systematic error for velocity and blood flow for representative data in umbilical vessels. While the basic idea of ng-PCMRI imaging for fast acquisition was proposed over two decades ago, its use has been confined to a few applications due to limited precision in high pulsatility flow conditions.^{17,24} Also, while these previous works focused on the application of ng-PCMRI in major arteries in adults, our study focused on assessing its applicability in fetal vessels in utero.

The flow in the umbilical artery and vein ranged from 68.4–378 ml/min and 61.8–420 ml/min (GA range: 24–39 5/7 weeks), respectively. The average flow measured in this study using the ng-PCMRI technique were 232 ± 92 ml/min in the umbilical vein and 203 ± 80 ml/min in the umbilical artery; these values were very similar to those reported by Lees et al²⁵ (vein 261 ± 98 ml/min; artery 226 ± 67 ml/min). The average normalized flow in the umbilical vein in our cohort of subjects was 155 ml/min/kg, similar to 160 ± 62 ml/min/kg previously reported using retrospective gating.²⁶ The average flow in the umbilical

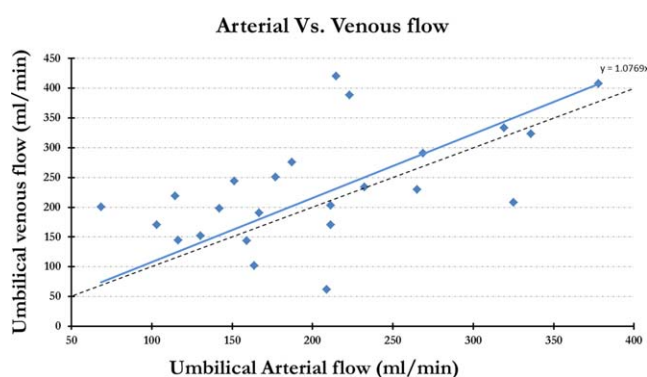


FIGURE 7: Combined umbilical arterial flow plotted across the corresponding venous flow.

artery was 140 ml/min/kg, which was within the range quoted in the previous studies (90–175 ml/min/kg).²⁷ While umbilical vein flow correlated well with the combined flow of the arteries, umbilical artery flow is seen to be underestimated. The average flow in the vein across all the subjects was greater than the average of the combined flow in the two umbilical arteries by $\sim 18\%$. This mismatch is comparable to that seen in a previous study.²⁵ This underestimation in the umbilical artery flow may be explained in part by their small size and the consequent partial voluming. At 33 weeks of gestation, the average area of the umbilical artery is $0.1 \pm 0.01 \text{ cm}^2$ (radius ~ 2 voxels) and that of the vein is $0.46 \pm 0.7 \text{ cm}^2$ (radius ~ 5 voxels).²⁵ Simulation results showed that for vessels of radius 2 to 3 pixels, the error in flow estimation could be as large as 10% for a given vessel. The corresponding error in a vessel of radius ~ 5 voxels (umbilical vein) is less than 2%. Thus, the total flow in the two umbilical arteries could be underestimated by a factor greater than 10%, which is observed in our data. These systematic errors due to the partial voluming are similar to what has been reported using conventional gated techniques.²⁰ Partial voluming leads to an error in both the quantified velocity as well as the area of the vessel, consequently leading to an error in the blood flow estimation. One way to minimize error in the final flow is by measuring the area by considering the outer radius of the vessel.²⁰ Following this guideline, we also used the outer radius of the vessel while evaluating the vessel CSA in the fetal data. The flow encoding in this study was only in the through plane (slice direction); however, the umbilical artery has a helical coil orientation, leading to averaging over the slice thickness or only measuring the component of flow perpendicular to the slice. While the same was not a concern for the vein, as they are homogeneous and the slice was positioned perpendicular to the umbilical cord.

The simulations included in this study only looked at the phase effects of the time-varying velocity pattern. But changes in velocity would also lead to changes in the time-of-flight effect of blood, and consequently the signal amplitude. Previous studies, however, have reported that the magnitude-induced variations in the flow quantification is low and can be reduced further using a low flip angle, relative to the Ernst angle.¹⁹ Due to the time-of-flight effect, the effective T_1 of blood for a 2D spoiled gradient echo imaging sequence depends on the slice thickness and average flow velocity. In the case of simulations and the in vivo data in the umbilical arteries, the average velocity was approximately $v = 15 \text{ cm/sec}$. This results in an effective T_1 for blood of $T_{1,eff} = 27 \text{ msec}$, for a slice thickness of 4 mm, and blood T_1 value of 1890 msec.²⁸ The corresponding Ernst angle for flowing blood, for the $TR = 14 \text{ msec}$ used in our sequence and simulations, is 58° . The flip angle of 15° used in our experiments is much lower than the Ernst angle. The signal from

flowing blood is more spin-density weighted in our in vivo experiments and in our simulation, and hence view-to-view variations in the blood signal are minimal/insignificant. In addition, the T_1 relaxation of the fetal blood is comparable to the adult blood,²⁹ and hence results from earlier studies can be readily extrapolated to fetal imaging.

Few previous studies have reported the use of MRI-based methods to quantify umbilical flow.^{30,31} These works were based on synthetic trigger approaches, where the data are oversampled and retrospectively sorted to reconstruct the images at different cardiac phases. However, this approach involves complex postprocessing, and limitations in the techniques preclude it from being used at early gestational ages.³¹ The use of image-based metric and periodicity constraints (modeled heart-rates) further imposes challenges in the reconstruction and quantification. We have shown that this ng-PCMRI approach can even be used in the second trimester of pregnancy. In ng-PCMRI, the V_{enc} can be reduced to improve the sensitivity of the measurements to the average velocity, while in pulse-gated PCMRI the V_{enc} must be maintained high to correspond to the systolic velocity rates. This reduces the sensitivity for diastolic velocity; on the other hand, in ng-PCMRI there would be no aliasing (phase-wraps) in the final phase images even if the instantaneous velocity during a few phase encode lines is greater than the V_{enc} as it encodes the average velocity.³²

There are a few limitations in the study design of the current feasibility study. The data presented here could not be systematically compared with the triggered/standard measurements and the measure of accuracy is based on simulation, internal validation (artery vs. vein), or comparison with literature values. Comparison with corresponding volumetric flow measures from Doppler US in the same cohort of fetuses could not be performed in this feasibility study. Furthermore, as the ng-PCMRI data were collected as part of a larger ongoing study, ng-PCMRI measurements from only a small cohort of subjects was possible. Systematic comparison of ng-PCMRI and Doppler US values in a larger cohort of subjects would be the focus of our future study.

In conclusion, the results of this study demonstrate the feasibility and applicability of nongated phase contrast MRI for in utero volumetric blood flow assessment in the human fetus. Fetal motion and poor SNR continue to be a challenge for the robust application of this in fetal imaging. Nevertheless, this approach is readily transferable to clinical diagnostic studies due to the ease of imaging and reconstruction. Potential to extend this approach beyond the umbilical cord to other fetal vessels exists, provided care is taken to avoid partial voluming and positioning the imaging slice perpendicular to the vessel. This approach in combination with other quantitative MRI tools can provide a more comprehensive understanding of the developmental

physiology and provide a sensitive biomarker for diagnosis of fetal distress.

Acknowledgments

Contract grant sponsor: STTR grant from the NHLBI, number 1R42HL112580-01A1; Contract grant sponsor: Perinatology Research Branch, Division of Obstetrics and Maternal-Fetal Medicine, Division of Intramural Research, Eunice Kennedy Shriver; Contract grant sponsor: National Institute of Child Health and Human Development, National Institutes of Health, U.S. Department of Health and Human Services (NICHD/NIH/DHHS); contract grant number: HHSN275201300006C.

The authors thank Anabela Trifan and the research staff at PRB for their help in volunteer recruitment. We also thank Dr. Wei Feng for the initial help with the sequence testing and Dr. Feifei Qu for help with article review.

References

1. Bhide A, Acharya G, Bilardo C, et al. ISUOG practice guidelines: use of Doppler ultrasonography in obstetrics. *Ultrasound Obstet Gynecol* 2013;41:233.
2. Kypros N, Giuseppe R, Kurt H, Renato X. Doppler ultrasound — Diploma in fetal medicine & ISUOG educational series. In: Nicolaidis K, ed. *Doppler in Obstetrics, ISUOG educational Series*. Campinas - SP Brazil; 2002.
3. Laurin J, Marsal K, Persson PH, Lingman G. Ultrasound measurement of fetal blood flow in predicting fetal outcome. *BJOG: Int J Obstet Gynaecol* 1987;94:940–948.
4. Baschat A, Gembruch U, Reiss I, Gortner L, Weiner C, Harman C. Relationship between arterial and venous Doppler and perinatal outcome in fetal growth restriction. *Ultrasound Obstet Gynecol* 2000;16:407–413.
5. Swillens A, Van Canneyt K, Segers P, Lovstakken L. The accuracy of volume flow measurements derived from pulsed wave Doppler: a study in the complex setting of forearm vascular access for hemodialysis. In: *2012 IEEE International Ultrasonics Symposium*. 2012. p. 1960–1963.
6. Gill RW. Measurement of blood flow by ultrasound: accuracy and sources of error. *Ultrasound Med Biol* 1985;11:625–641.
7. Blanco P. Volumetric blood flow measurement using Doppler ultrasound: concerns about the technique. *J Ultrasound* 2015;18:201–204.
8. Quinn TM, Hubbard AM, Adzick NS. Prenatal magnetic resonance imaging enhances fetal diagnosis. *J Pediatr Surg* 1998;33:553–558.
9. Breysem L, Bosmans H, Dymarkowski S, et al. The value of fast MR imaging as an adjunct to ultrasound in prenatal diagnosis. *Eur Radiol* 2003;13:1538–1548.
10. Frayne R, Steinman DA, Rutt BK, Ethier CR. Accuracy of MR phase contrast velocity measurements for unsteady flow. *J Magn Reson Imaging* 1995;5:428–431.
11. Oktar S, Yücel C, Karaosmanoglu D, et al. Blood-flow volume quantification in internal carotid and vertebral arteries: comparison of 3 different ultrasound techniques with phase-contrast MR imaging. *Am Neuroradiol* 2006;27:363–369.
12. Jiang J, Strother C, Johnson K, et al. Comparison of blood velocity measurements between ultrasound Doppler and accelerated phase-contrast MR angiography in small arteries with disturbed flow. *Phys Med Biol* 2011;56:1755.
13. Zhu MY, Jaeggi E, Roy CW, Macgowan CK, Seed M. Reduced combined ventricular output and increased oxygen extraction fraction in a fetus with complete heart block demonstrated by MRI. *HeartRhythm Case Rep* 2016;2:164–168.
14. Seed M, van Amerom JF, Yoo S-J, et al. Feasibility of quantification of the distribution of blood flow in the normal human fetal circulation using CMR: a cross-sectional study. *J Cardiovasc Magn Reson* 2012;14:1.
15. Schoennagel BP, Remus CC, Yamamura J, et al. Fetal blood flow velocimetry by phase-contrast MRI using a new triggering method and comparison with Doppler ultrasound in a sheep model: a pilot study. *Magn Reson Mater Phys Biol Med* 2014;27:237–244.
16. Kording F, Yamamura J, Lund G, et al. Doppler ultrasound triggering for cardiovascular MRI at 3T in a healthy volunteer study. *Magn Reson Med* 2016 [Epub ahead of print].
17. Bakker C, Kouwenhoven M, Hartkamp M, Hoogeveen R, Mali W, et al. Accuracy and precision of time-averaged flow as measured by nontriggered 2D phase-contrast MR angiography, a phantom evaluation. *Magn Reson Imaging* 1995;13:959–965.
18. Hangiandreou NJ, Rossman PJ, Riederer SJ. Analysis of MR phase-contrast measurements of pulsatile velocity waveforms. *J Magn Reson Imaging* 1993;3:387–394.
19. Yeh S-Y, Forsythe A, Hon EH. Quantification of fetal heart beat-to-beat interval differences. *Obstet Gynecol* 1973;41:355–363.
20. Jiang J, Kokeny P, Ying W, Magnano C, Zivadinov R, Haacke EM. Quantifying errors in flow measurement using phase contrast magnetic resonance imaging: comparison of several boundary detection methods. *Magn Reson Imaging* 2015;33:185–193.
21. Hadlock FP, Harrist R, Sharman RS, Deter RL, Park SK. Estimation of fetal weight with the use of head, body, and femur measurements—a prospective study. *Am J Obstet Gynecol* 1985;151:333–337.
22. Neelavalli J, Krishnamurthy U, Jella PK, et al. Magnetic resonance angiography of fetal vasculature at 3.0 T. *Eur Radiol* 2016;26:4570–4576.
23. Feng W, Utraiainen D, Trifan G, et al. Characteristics of flow through the internal jugular veins at cervical C2/C3 and C5/C6 levels for multiple sclerosis patients using MR phase contrast imaging. *Neurol Res* 2012;34:802–809.
24. Bakker CJ, Hoogeveen RM, Viergever MA. Construction of a protocol for measuring blood flow by two-dimensional phase-contrast MRA. *J Magn Reson Imaging* 1999;9:119–127.
25. Lees C, Albaiges G, Deane C, Parra M, Nicolaidis K. Assessment of umbilical arterial and venous flow using color Doppler. *Ultrasound Obstet Gynecol* 1999;14:250–255.
26. Seed M, van Amerom JF, Yoo S-J, et al. Feasibility of quantification of the distribution of blood flow in the normal human fetal circulation using CMR: a cross-sectional study. *J Cardiovasc Magn Reson* 2012;14:79.
27. Goldkrand J, Pettigrew C, Lentz S, Clements S, Bryant J, Hodges J. Volumetric umbilical artery blood flow: comparison of the normal versus the single umbilical artery cord. *J Matern Fetal Med* 2001;10:116–121.
28. De Vis J, Hendrikse J, Groenendaal F, et al. Impact of neonate haematocrit variability on the longitudinal relaxation time of blood: Implications for arterial spin labelling MRI. *NeuroImage Clin* 2014;4:517–525.
29. Portnoy S, Osmond M, Zhu MY, Seed M, Sled JG, Macgowan CK. Relaxation properties of human umbilical cord blood at 1.5 Tesla. *Magn Reson Med* 2016 [Epub ahead of print].
30. Tsai-Goodman B, Zhu MY, Al-Rujaib M, Seed M, Macgowan CK. Foetal blood flow measured using phase contrast cardiovascular magnetic resonance—preliminary data comparing 1.5 T with 3.0 T. *J Cardiovasc Magn Reson* 2015;17:30.
31. Prsa, M, Sun L, van Amerom J, et al. Reference ranges of blood flow in the major vessels of the normal human fetal circulation at term by phase-contrast magnetic resonance imaging: Clinical perspective. *Circ Cardiovasc Imaging* 2014;7:663–670.
32. Enzmann DR, Marks MP, Pelc NJ. Comparison of cerebral artery blood flow measurements with gated cine and ungated phase-contrast techniques. *J Magn Reson Imaging* 1993;3:705–712.